MATERIALS AND METHODS

Strains and cell culture: The *M. smegmatis* strain mc^2155, augmented with a kanamycin resistance-integrating vector pMV306, was used in this study (gift of Chris Sassetti and Kadamba Papavinasasundaram). The cells were cultured in 7H9 media supplemented with 0.2% glycerol, 0.05% Tween-80, 10% OADC, and 25 μg/ml kanamycin. *M. smegmatis* were grown to log phase and filtered through a 10 μm filter to achieve a single cell suspension. The *M. tuberculosis* strain H37Rv was cultured in 7H9 supplemented as described above but without kanamycin. The leucine/pantothenate *M. tuberculosis* auxotroph (*M. tuberculosis* Δ*leu* Δ*panCD*) was cultured in 7H9 as described for *M. tuberculosis* and additionally supplemented with 50 μg/ml leucine (Sigma-Aldrich) and 24 μg/ml pantothenate (Sigma-Aldrich) *(31)*. This strain was constructed by Sampson et al. as a candidate vaccine strain but may be used in a biosafety level 2 facility *(31)*. The *E. coli* strain DH5α was grown in LB broth. All cells were grown and imaged at 37°C.

Microfluidic device: Microfluidic devices were made of polydimethylsiloxane (PDMS) bonded to glass substrates using soft lithography techniques *(32)*. Briefly, the desired pattern was photolithographically defined by using a Mylar mask printed at 40,000 dpi and created by employing negative photoresist (SU-8, MicroChem) patterned on silicon wafers. This process created masters with two-layer features. The first SU-8 was made to a height of approximately 0.8−0.9 μm and defined the side channels and chambers where mycobacteria are loaded, whereas the second layer was deposited to a height ranging 10−17 μm to form the main microfluidic feeding channel and serpentine mixer, where appropriate. The heights of SU-8 features on the masters were measured with a surface profilometer (Dektak ST System Profilometer, Veeco Instruments Inc.). The masters were then used as molds, on which PDMS prepolymer mixed with crosslinker at 10:1 weight ratio was poured, degassed, and allowed to cure in a conventional oven at 65 ºC for at least 24 h. The cured PDMS replicas were then removed from the molds and fluid inlet and outlet ports were punched with a sharpened flat-tip needle. Finally, the PDMS replicas were subjected to a brief oxygen plasma treatment, and bonded to glass cover slips to obtain the final devices.

Microscopy: Time-lapse images were acquired using a DeltaVision PersonalDV microscope with an automated stage enclosed in an environmental chamber warmed to 37^{o}C (Applied Precision, Inc.). Images were acquired with 60x- (Plan APO NA 1.42) and 100x- (Plan APO NA 1.40) oil objectives for *M. smegmatis* and *M. tuberculosis*, respectively. Cells were illuminated with the InsightSSI Solid State Illumination system (461-489 nm; Applied Precision, Inc.) and recorded with a CoolSnap HQ2 camera (Photometric). Focus was maintained using the Ultimate Focus System (Applied Precision, Inc.). Images were acquired every ten minutes for 18-24 hours for *M. smegmatis* and up to 72 hours for the leucine/pantothenate *M. tuberculosis* auxotroph. Images were acquired every minute for two hours with the 60x objective (above) for *E. coli*.

Image processing and analysis: Images were saved in the Softworx format (Applied Precision, Inc.) and annotated in ImageJ and ObjectJ *(33, 34)*. Custom python and Matlab programs were used to analyze the annotations (The Mathworks). The brightness and contrast were adjusted linearly and identically across the each image in a series. Ten microcolonies of *M. smegmatis* (totaling 322 cells) were analyzed for this study. Our annotation procedure produced similar distribution of elongation rates to published rates when used to measure *E. coli* elongation rate *(35)*.

Cell wall labeling: Cells were pelleted and washed with PBS with 0.2% Tween 20 (PBST) and resuspended in PBST in 1/10 of the culture volume. Alexa Fluor 488 carboxylic acid succinimidyl ester was added to a final concentration of 0.05 mg/ml and gently mixed (Invitrogen). The cells were pelleted immediately, washed in PBST and resuspended in culture media. This staining process did not alter growth rate (fig. S5A). *M. tuberculosis* cells were fixed for one hour in 4% parafomaldehyde before removal from the biosafety level 3 facility. Alexa568-conjugated vancomycin (Van-Alexa) was generously provided by Robert Husson and Mushtaq Mir *(36)*. *M. smegmatis* cells were grown for 2.5 hours in the microfluidic device before staining with 5 μg/mL Van-Alexa for two hours. The cells were images with an mCherry-optimized filter set after flowing regular growth media for one hour.

Antibiotic treatment: *M. smegmatis* were grown in a microfluidic device for eight hours to establish microcolonies before treatment for eight hours at the minimal inhibitory concentration of meropenem (2.3 mM), D-cycloserine (0.04 mg/ml), isoniazid (25 μM), and rifampicin (50

μM), as determined using an Alamar blue assay (*(37)*; Sigma-Aldrich). The cells recovered in normal growth media for eight hours. The cells were grown in a modified microfluidic device. The device was outfitted with two inlets (one for normal media and one for media with antibiotics; only one inlet was used at a time) and the shallow channels ended with a 60 μm diameter circular "room" that enabled us to visualize the recovery of cells more readily. The channels leading up to the room were 100-200 μm long, 10-16 μm wide, and the room and the channels were 1 μm tall.

Statistical analysis: Statistical analysis was performed using the Statistics Toolbox in Matlab 2010a (The Mathworks). Distributions were compared to the null hypothesis using a t-test and two distribution were compared to each other using a two-sample F test for equal variance where not specified.

REFERENCES AND NOTES

1. D. L. Cohn, B. J. Catlin, K. L. Peterson, F. N. Judson, J. A. Sbarbaro, A 62-dose, 6-month therapy for pulmonary and extrapulmonary tuberculosis. A twice-weekly, directly observed, and cost-effective regimen, *Ann. Intern. Med* **112**, 407-415 (1990).

2. G. Elzinga, M. C. Raviglione, D. Maher, Scale up: meeting targets in global tuberculosis control, *Lancet* **363**, 814-819 (2004).

3. R. M. McCune, F. M. Feldmann, H. P. Lambert, W. McDermott, Microbial persistence. I. The capacity of tubercle bacilli to survive sterilization in mouse tissues, *J. Exp. Med* **123**, 445-468 (1966).

4. L. E. Connolly, P. H. Edelstein, L. Ramakrishnan, Why Is Long-Term Therapy Required to Cure Tuberculosis?, *PLoS Med* **4**, e120 (2007).

5. Materials and methods are available as supporting material on *Science* online.

6. E. C. Hett, E. J. Rubin, Bacterial growth and cell division: a mycobacterial perspective, *Microbiol. Mol. Biol. Rev* **72**, 126-156, table of contents (2008).

7. P. Farnia et al., Growth and cell-division in extensive (XDR) and extremely drug resistant (XXDR) tuberculosis strains: transmission and atomic force observation, *Int J Clin Exp Med* **3**, 308-314 (2010).

8. B. Singh, J. Ghosh, N. M. Islam, S. Dasgupta, L. A. Kirsebom, Growth, cell division and sporulation in mycobacteria, *Antonie Van Leeuwenhoek* **98**, 165-177 (2010).

9. N. R. Thanky, D. B. Young, B. D. Robertson, Unusual features of the cell cycle in mycobacteria: polar-restricted growth and the snapping-model of cell division, *Tuberculosis (Edinb)* **87**, 231-236 (2007).

10. M. Mentinova, S. A. McLuckey, Covalent Modification of Gaseous Peptide Ions with N-Hydroxysuccinimide Ester Reagent Ions, *Journal of the American Chemical Society* **132**, 18248-18257 (2010).

11. W. Messer, The bacterial replication initiator DnaA. DnaA and oriC, the bacterial mode to initiate DNA replication, *FEMS Microbiol. Rev* **26**, 355-374 (2002).

12. A. Løbner-Olesen, K. Skarstad, F. G. Hansen, K. von Meyenburg, E. Boye, The DnaA protein determines the initiation mass of Escherichia coli K-12, *Cell* **57**, 881-889 (1989).

13. A. Sveiczer, B. Novak, J. M. Mitchison, The size control of fission yeast revisited, *J. Cell. Sci* **109 (Pt 12)**, 2947-2957 (1996).

14. S. Di Talia, J. M. Skotheim, J. M. Bean, E. D. Siggia, F. R. Cross, The effects of molecular noise and size control on variability in the budding yeast cell cycle, *Nature* **448**, 947-951 (2007).

15. L. Shapiro, H. H. McAdams, R. Losick, Generating and Exploiting Polarity in Bacteria, *Science* **298**, 1942 -1946 (2002).

16. Y. E. Chen et al., Spatial gradient of protein phosphorylation underlies replicative asymmetry in a bacterium, *Proc. Natl. Acad. Sci. U.S.A* **108**, 1052-1057 (2011).

17. K. Carniol, S. Ben-Yehuda, N. King, R. Losick, Genetic dissection of the sporulation protein SpoIIE and its role in asymmetric division in Bacillus subtilis, *J. Bacteriol* **187**, 3511-3520 (2005).

18. J.-W. Veening et al., Bet-hedging and epigenetic inheritance in bacterial cell development, *Proc. Natl. Acad. Sci. U.S.A* **105**, 4393-4398 (2008).

19. S. Ben-Yehuda, R. Losick, Asymmetric cell division in B. subtilis involves a spiral-like intermediate of the cytokinetic protein FtsZ, *Cell* **109**, 257-266 (2002).

20. E. J. Stewart, R. Madden, G. Paul, F. Taddei, Aging and death in an organism that reproduces by morphologically symmetric division, *PLoS Biol* **3**, e45 (2005).

21. D. Huh, J. Paulsson, Non-genetic heterogeneity from stochastic partitioning at cell division, *Nat Genet* **43**, 95-100 (2011).

22. C. G. Tsokos, B. S. Perchuk, M. T. Laub, A dynamic complex of signaling proteins uses polar localization to regulate cell-fate asymmetry in Caulobacter crescentus, *Dev. Cell* **20**, 329-341 (2011).

23. P. H. Viollier, N. Sternheim, L. Shapiro, Identification of a localization factor for the polar positioning of bacterial structural and regulatory proteins, *Proc. Natl. Acad. Sci. U.S.A* **99**, 13831-13836 (2002).

24. R. B. Jensen, S. C. Wang, L. Shapiro, Dynamic localization of proteins and DNA during a bacterial cell cycle, *Nat. Rev. Mol. Cell Biol* **3**, 167-176 (2002).

25. P. H. Viollier, N. Sternheim, L. Shapiro, A dynamically localized histidine kinase controls the asymmetric distribution of polar pili proteins, *EMBO J* **21**, 4420-4428 (2002).

26. Y. Chai, T. Norman, R. Kolter, R. Losick, An epigenetic switch governing daughter cell separation in Bacillus subtilis, *Genes & Development* **24**, 754 -765 (2010).

27. N. Q. Balaban, J. Merrin, R. Chait, L. Kowalik, S. Leibler, Bacterial Persistence as a Phenotypic Switch, *Science* **305**, 1622 -1625 (2004).

28. P. Bordes et al., SecB-like chaperone controls a toxin-antitoxin stress-responsive system in Mycobacterium tuberculosis, *Proc. Natl. Acad. Sci. U.S.A* **108**, 8438-8443 (2011).

29. K. Lewis, Persister cells, dormancy and infectious disease, *Nat Rev Micro* **5**, 48-56 (2007).

30. C.-M. Kang, S. Nyayapathy, J.-Y. Lee, J.-W. Suh, R. N. Husson, Wag31, a homologue of the cell division protein DivIVA, regulates growth, morphology and polar cell wall synthesis in mycobacteria, *Microbiology (Reading, Engl.)* **154**, 725-735 (2008).

31. S. L. Sampson et al., Protection elicited by a double leucine and pantothenate auxotroph of Mycobacterium tuberculosis in guinea pigs, *Infect. Immun* **72**, 3031-3037 (2004).

32. Y. Xia, G. M. Whitesides, SOFT LITHOGRAPHY, *Annu. Rev. Mater. Sci.* **28**, 153-184 (1998).

33. Rasband, W.S., *ImageJ* (U. S. National Institutes of Health, Bethesda, Maryland, USA, 2007; http://imagej.nih.gov/ij/).

34. Vischer, Norbert, Nastase, Stelian, *ObjectJ* (University of Amsterdam; http://simon.bio.uva.nl/objectj/index.html).

35. A. B. Lindner, R. Madden, A. Demarez, E. J. Stewart, F. Taddei, Asymmetric segregation of protein aggregates is associated with cellular aging and rejuvenation, *Proc. Natl. Acad. Sci. U.S.A* **105**, 3076-3081 (2008).

36. C.-M. Kang, S. Nyayapathy, J.-Y. Lee, J.-W. Suh, R. N. Husson, Wag31, a homologue of the cell division protein DivIVA, regulates growth, morphology and polar cell wall synthesis in mycobacteria, *Microbiology* **154**, 725-735 (2008).

37. S. G. Franzblau et al., Rapid, Low-Technology MIC Determination with Clinical Mycobacterium tuberculosis Isolates by Using the Microplate Alamar Blue Assay, *J. Clin. Microbiol.* **36**, 362-366 (1998).

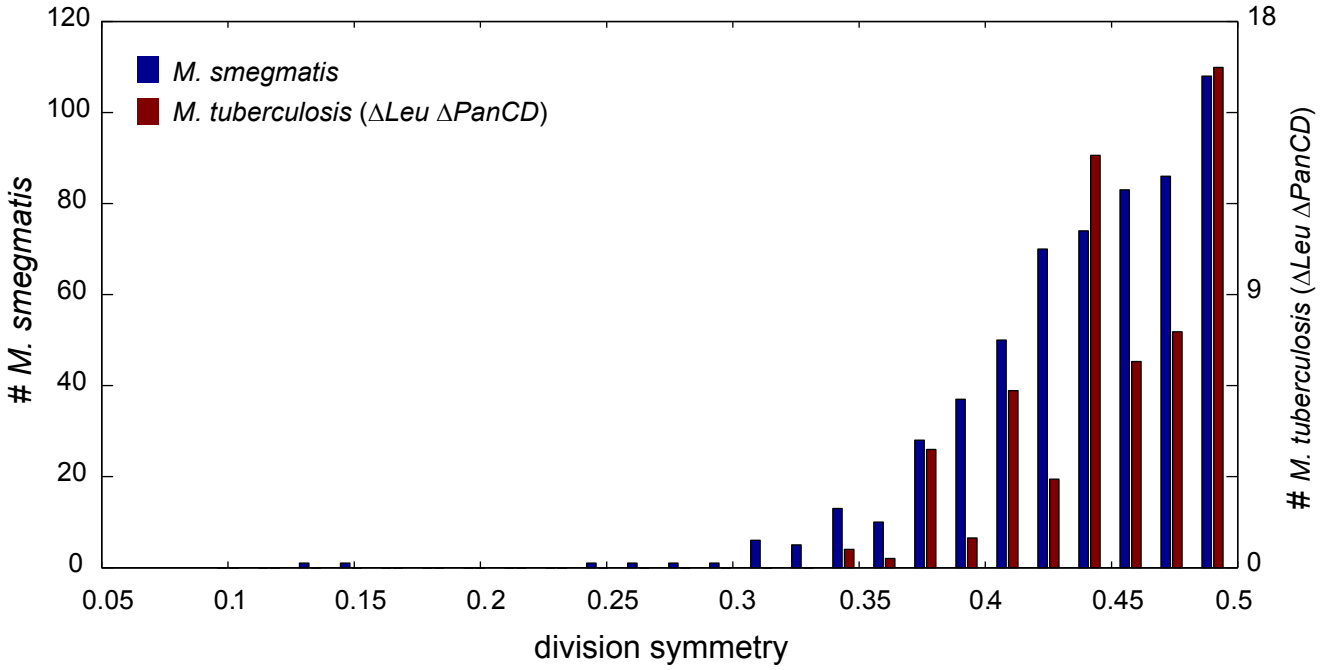

Figure S1. Division symmetry is similar in *M. tuberculosis* and *M. smegmatis.* *M. tuberculosis* Δ*Leu* Δ*PanCD* and *M. smegmatis* were grown and imaged on an enclosed 4% agarose pad in supplemented 7H9 media *(5)*. The division symmetry of recently divided sister cells are plotted as depicted in Figure 1D.

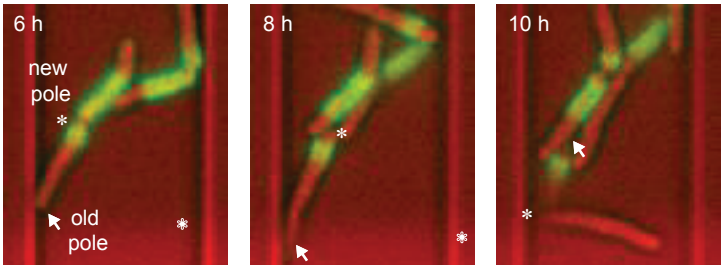

Figure S2. Cells inheriting the mother's growth pole continue to elongate from that growing pole. Time-lapse images of a representative *M. smegmatis* cell that inherits a small section of the pulse-labeled cell wall. This cell inherits the mother's growing pole and continues to elongate from the same pole before dividing (between 8 and 10 h).

A

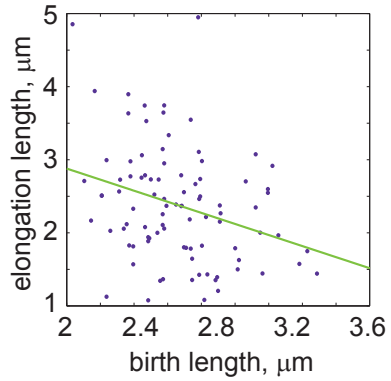

B

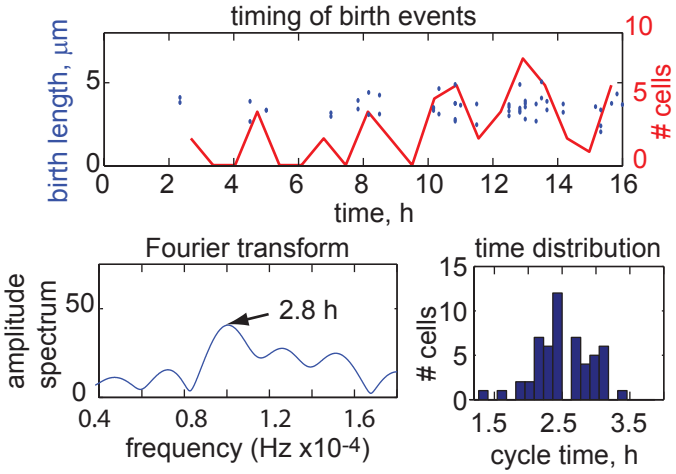

C

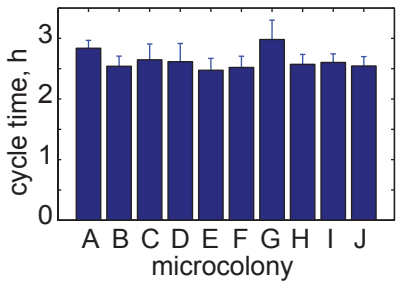

Figure S3. The cell division cycle is governed by time in *M. smegmatis*. (A) Birth length and elongation length, which is defined as the length that the cell elongates between birth and division, are negatively correlated for 102 *E. coli* cells (regression slope of -0.75). (B) Characterization of the timing of birth events. A second representative microcolony is shown here (the first example is illustrated in Figure 4B). (C) Cell cycle times based on the population mean (from the time domain) for ten microcolonies. The error bars represent the standard deviation. Microcolonies A and G had significantly different cell cycle times than B, E, F, H, I, and J ($p<0.05$ by a rank sum Mann-Whitney test).

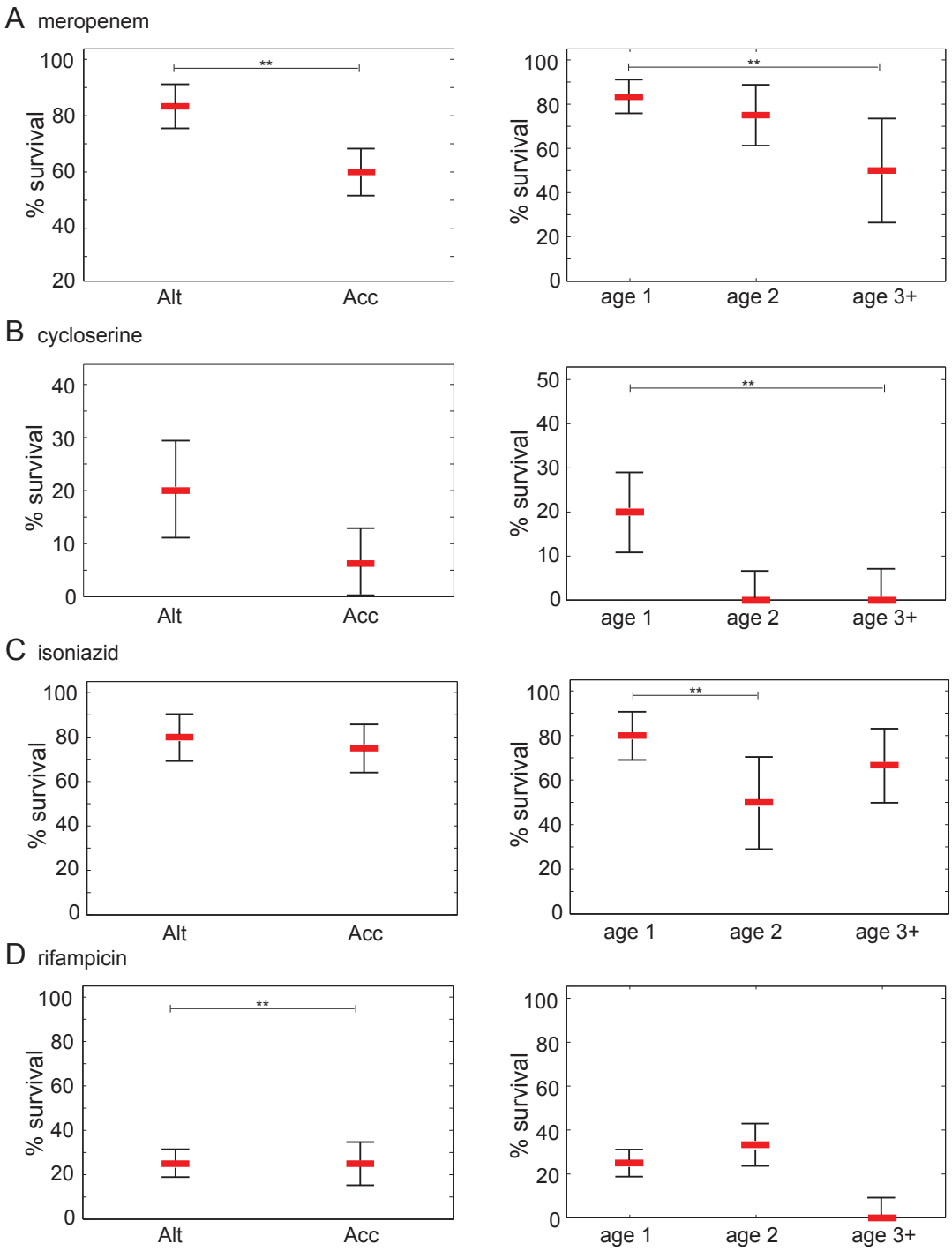

Figure S4. Alternator and accelerator cells and individual microcolonies are differentially susceptible to different classes of antibiotics. Percent survival post-treatment is plotted as the median of survival per microcolony (red) with error bars denoting 95% confidence intervals for accelerators and alternators (left), and growth pole ages (right). *M. smegmatis* cells were treated with minimal inhibitory concentrations of (A) meropenem, (B) cycloserine, (C) isoniazid, and (D) rifampicin (2.3 mM, 0.04 mg/ml, 25 μM, and 50 μM, respectively). Asterisks (**) denote $p<0.05$ by a Mann-Whitney rank sum test, indicating that the medians were derived from statistically different distributions.

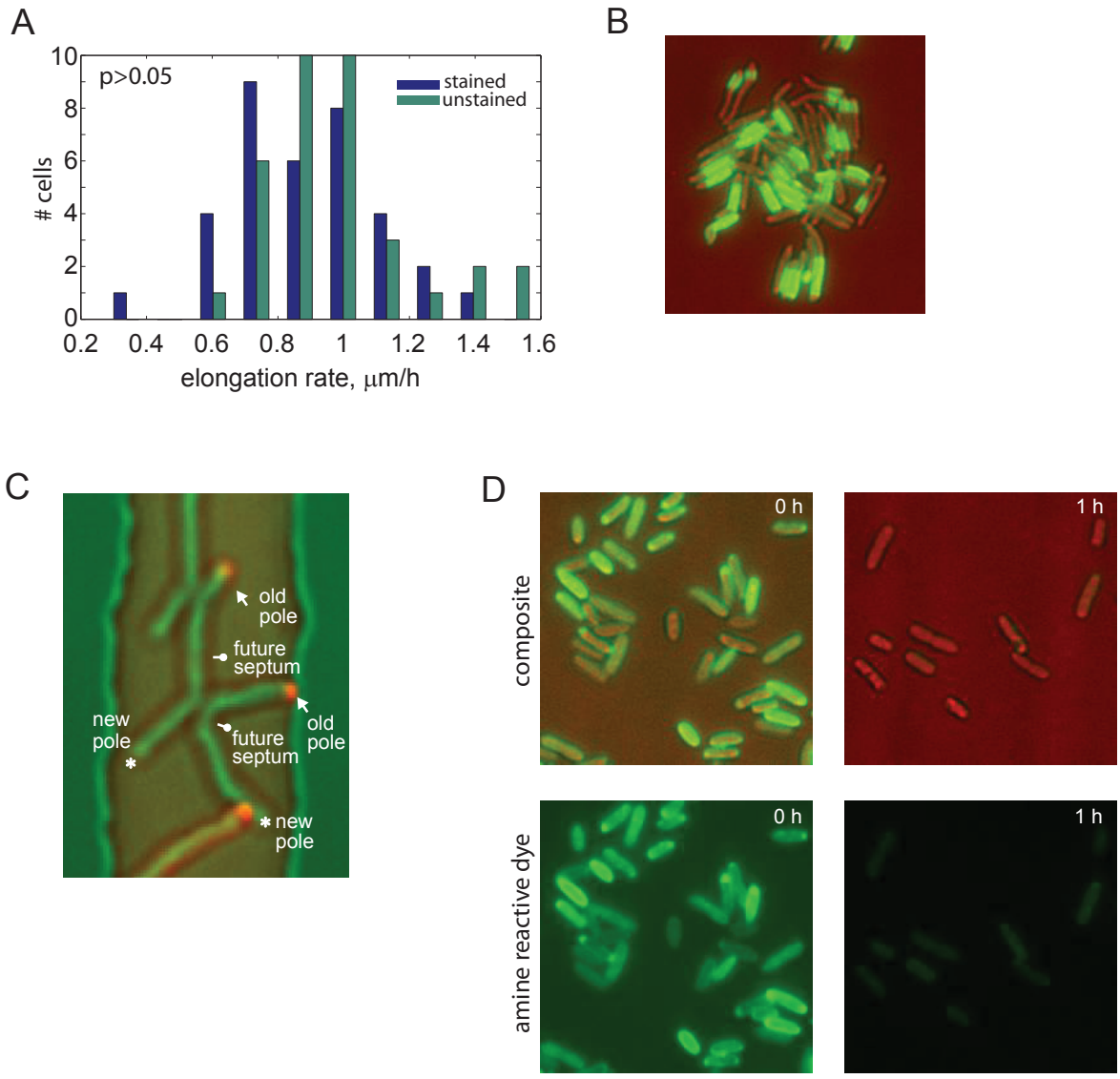

Figure S5. Amine reactive dye stains the cell wall without affecting growth rate. (A) Distribution of the elongation rates of 35 *M. smegmatis* cells that are stained or unstained with amine reactive dye. The growth rates are similar (p>0.05). (B) Image of *M. smegmatis* cells grown in suspension and pulse-labeled. (C) Representative image of *M. smegmatis* cells briefly labeled with Vanc-Alexa568 (red), localized primarily to the old (growing) pole (arrow). The new pole, old pole, and anticipated site of septation were determined by time-lapse microscopy. The bright field image is pseudo-colored green. (D) Images of *E. coli* cells pulse-labeled with amine reactive dye immediately after the labeling and one hour later. The dye is shown in green and the bright field image is pseudo-colored red. The dye diffuses after a few generations of recovery, in contrast to *M. smegmatis*.